

## Reorientation Transition in Single-Domain (Ga,Mn)As

K-Y. Wang,<sup>1</sup> M. Sawicki,<sup>2,\*</sup> K.W. Edmonds,<sup>1</sup> R.P. Campion,<sup>1</sup> S. Maat,<sup>3</sup>  
C.T. Foxon,<sup>1</sup> B.L. Gallagher,<sup>1</sup> and T. Dietl<sup>2,4</sup>

<sup>1</sup>*School of Physics and Astronomy, University of Nottingham, Nottingham NG7 2RD, UK*

<sup>2</sup>*Institute of Physics, Polish Academy of Sciences,  
al. Lotników 32/46, PL-02668 Warszawa, Poland*

<sup>3</sup>*Hitachi Global Storage Technologies, San Jose Research Center,  
650 Harry Road, San Jose, California 95120, USA*

<sup>4</sup>*ERATO Semiconductor Spintronics Project, al. Lotników 32/46, PL-02668 Warszawa, Poland  
and Institute of Theoretical Physics, Warsaw University, PL-00681 Warszawa, Poland*

(Dated: July 17, 2021)

We demonstrate that the interplay of in-plane biaxial and uniaxial anisotropy fields in (Ga,Mn)As results in a magnetization reorientation transition and an anisotropic AC susceptibility which is fully consistent with a simple single domain model. The uniaxial and biaxial anisotropy constants vary respectively as the square and fourth power of the spontaneous magnetization across the whole temperature range up to  $T_C$ . The weakening of the anisotropy at the transition may be of technological importance for applications involving thermally-assisted magnetization switching.

PACS numbers: 75.50.Pp, 75.30.Gw, 75.70.-i

Following the emergence of the ferromagnetic semiconductor (Ga,Mn)As as a test bed for semiconductor spintronics, intensive efforts have been dedicated to its materials development [1]. In early studies [2] it was concluded that (Ga,Mn)As suffered from very high compensation, and a large magnetization deficit leading to concern that there were fundamental problems with this, and by implication other, dilute ferromagnetic semiconductors. However it has now been established that the observed non-ideal behavior arose from extrinsic defects [3]. Studies of carefully prepared samples have now shown that compensation can be very low [4] and the magnetic moment per Mn can attain close to its free ion value [5]. It is now generally accepted that (Ga,Mn)As is a well-behaved mean field ferromagnet with a Curie temperature  $T_C$  that increases linearly with substitutional Mn concentration [6]. Furthermore, (Ga,Mn)As films generally show excellent micromagnetic properties that can be described both phenomenologically and on the basis of microscopic theories [7, 8].

However, some uncertainties remain about the intrinsic sample homogeneity, and to what extent this may influence the magnetic properties. It has been suggested that microscopic phase segregation may be energetically favorable leading to clustering of Mn atoms [9, 10]. Very recently it has been argued that DC and AC magnetometry results indicate segregation into two distinct ferromagnetic phases [11]. In this paper we establish a unified description of the DC and AC magnetic properties of (Ga,Mn)As and show that features interpreted as evidence for mixed phases in fact arise from a single-domain reorientation transition, which further establishes the excellent micromagnetic properties of this system, and which may have technological applications.

It is generally accepted that the ferromagnetic Mn-Mn interaction in (Ga,Mn)As is mediated by band holes, whose Kohn-Luttinger amplitudes are primarily built up of As  $4p$  orbitals. Since in semiconductors the Fermi energy is usually smaller than the spin-orbit energy, the confinement or strain-induced anisotropy of the valence band can lead to sizeable anisotropy of spin properties. (Ga,Mn)As grown on GaAs(001) is under compressive strain, which for relatively low compensation leads to magnetic easy axes along the in-plane  $\langle 100 \rangle$  directions. Quantitative calculations within the mean field Zener model describe the experimental values of the strain-induced anisotropy field with an accuracy better than a factor of two [7, 8]. It has also been realized that a uniaxial anisotropy, breaking the symmetry between in-plane  $[110]$  and  $[1\bar{1}0]$  directions, is required for a satisfactory description of the in-plane magnetization [12, 13, 14, 15, 16, 17]. These orientations are equivalent in the bulk and the microscopic origin remains unclear, however the observed behavior is consistent the mean field Zener model if an additional symmetry-breaking strain is introduced [17].

Phenomenologically, the magnetic energy can be described as:

$$E = -K_C \sin^2(2\theta)/4 + K_U \sin^2(\theta) - MH \cos(\varphi - \theta), \quad (1)$$

where  $K_C$  and  $K_U$  are the lowest order biaxial and uniaxial anisotropy constants,  $H$  is the external field,  $M$  the magnetization, and  $\theta$  and  $\varphi$  are the angle of  $M$  and  $H$  to the  $[1\bar{1}0]$  direction. This simple model describes experimental ferromagnetic resonance [15], magnetotransport [13] and magneto-optical [14] data remarkably well, indicating that, at least away from the reversal fields, macroscopically large (Ga,Mn)As films tend to align in a single

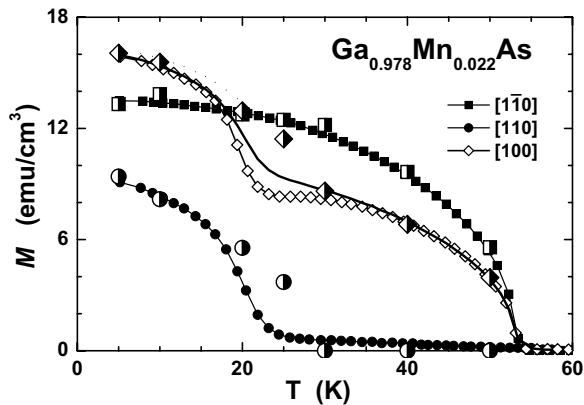


FIG. 1: Remnant magnetization along  $[1\bar{1}0]$ ,  $[110]$ , and  $[100]$  axes versus increasing temperature; (line) remnant magnetization along  $[100]$  extracted from the  $[1\bar{1}0]$  and  $[110]$  curves assuming single-domain behavior; (corresponding half-filled symbols) remnant magnetization calculated from equation (1) using the anisotropy constants obtained from the analysis of  $M(H)$  loops measured at selected temperatures.

domain state. However, the biaxial and uniaxial terms may each have a different dependence on the magnetization, so that a complicated temperature-dependence of the magnetic anisotropy is expected [18]. In particular, at a temperature where  $K_U = K_C$  the system should undergo a 2nd order magnetic easy axis reorientation transition from the biaxial-dominated case when  $K_U < K_C$ , to a uniaxial realm when  $K_U > K_C$ . In this paper we extract the temperature-dependence of  $K_U$  and  $K_C$  for a (Ga,Mn)As film using equation (1), and show that the observed transition of the in-plane anisotropy from biaxial to uniaxial is consistent with these values. Furthermore, we show that the reorientation transition gives rise to a peak in the temperature-dependence of the AC susceptibility well below  $T_C$ , even for a well-behaved single-phase sample, due to cancellation of anisotropy contributions. This can be distinguished from a ferromagnetic-to-paramagnetic transition by its dependence on the applied magnetic field direction.

50nm (Ga,Mn)As epilayers were grown by molecular beam epitaxy using  $\text{As}_2$ . Full details of the growth are given elsewhere [19]. The Mn concentration  $x$  is determined by x-ray diffraction and secondary ion mass spectrometry. We focus on results for a sample with  $x=0.022$ , but qualitatively similar magnetic properties are observed for as-grown samples with  $x=0.056$  and  $x=0.09$ . The hole concentration for this sample, determined by low-temperature high-field Hall effect measurements, is  $3.5 \times 10^{20} \text{ cm}^{-3}$ . SQUID magnetometry is used to determine the projected magnetization and AC susceptibility along the measurement axis, which is parallel to the applied magnetic field.

Figure 1a shows the measured projections of the remnant magnetization along the  $[110]$ ,  $[1\bar{1}0]$  and  $[100]$  direc-

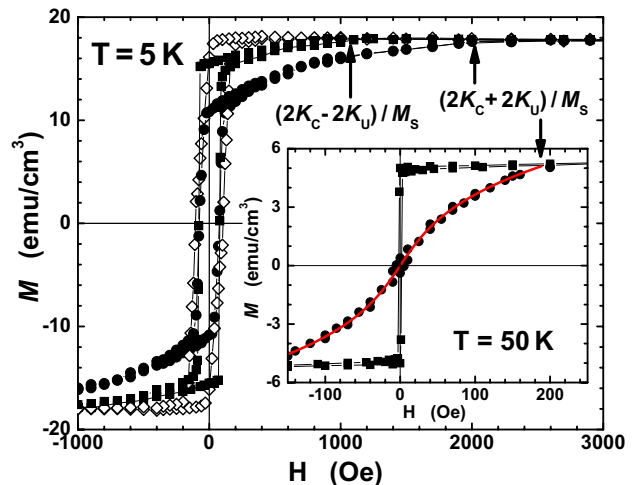


FIG. 2: Symbols as in Fig. 1.  $M(H)$  loops along the  $[1\bar{1}0]$ ,  $[110]$  and  $[100]$  axes at 5 K, with the arrows indicating the intersection points which are used to obtain  $K_U$  and  $K_C$  at low temperature. (inset)  $M(H)$  loops along the  $[1\bar{1}0]$  and  $[110]$  axes at 50 K, plus the fit to the hard axis curve used to obtain  $K_U$  and  $K_C$ . The arrow indicates the intersection point for uniaxial hard axis measurement.

tions,  $M_{[110]}$ ,  $M_{[1\bar{1}0]}$ , and  $M_{[100]}$ , for increasing temperature, recorded after cooling the sample through  $T_C$  under a 1000 Oe field. The trapped field in the magnet during these measurements is around 0.1 Oe. At low temperatures, the easy axes are close to the in-plane  $[100]$  and  $[010]$  orientations, while the uniaxial anisotropy favoring the  $[1\bar{1}0]$  orientation emerges with increasing temperature. Above around 30 K the remnant magnetization is fully aligned with the  $[1\bar{1}0]$  direction:  $M_{[100]}$  is smaller than  $M_{[1\bar{1}0]}$  by  $\cos(45^\circ)$ , while  $M_{[110]}$  is close to zero. If the sample is in a single domain state throughout these measurements, then  $M_{[100]}$  should be given by  $M_S \cos(45^\circ - \theta)$ , where  $\theta = \arctan(M_{[110]}/M_{[1\bar{1}0]})$ , and  $M_S^2 = M_{[110]}^2 + M_{[1\bar{1}0]}^2$ . As shown in Fig. 1a, this is in good agreement with the measured  $M_{[100]}$  over most of the temperature range with the only small deviation observed in the region close to the transition between biaxial and uniaxial anisotropy, at around 25 K. This compliance with simple geometrical considerations is a strong indication that the system behaves as a single, uniform domain, so that Eq. 1 can be used to extract the anisotropy constants  $K_C$  and  $K_U$ .

The dependence of  $M_{[110]}$ ,  $M_{[1\bar{1}0]}$ , and  $M_{[100]}$  on external magnetic field can be obtained by minimizing the energy given by Eq. 1 with respect to  $\theta$ . For the uniaxial easy  $[1\bar{1}0]$  axis this gives:  $H = -2(K_U + K_C)M_{[1\bar{1}0]}/M_S^2 + 4K_C M_{[1\bar{1}0]}^3/M_S^4$  for  $K_C > K_U$ , or  $M_{[1\bar{1}0]} = \text{sgn}(H)M_S$  for  $K_C < K_U$ ; while for the uniaxial hard  $[110]$  axis, the expression is  $H = 2(K_U - K_C)M_{[110]}/M_S^2 + 4K_C M_{[110]}^3/M_S^4$ . The simplest way to obtain  $K_C$  and  $K_U$  is by fitting the  $[110]$  magnetization curve to this expression. Such a fit is shown in the inset to Fig. 2. However, at low tem-

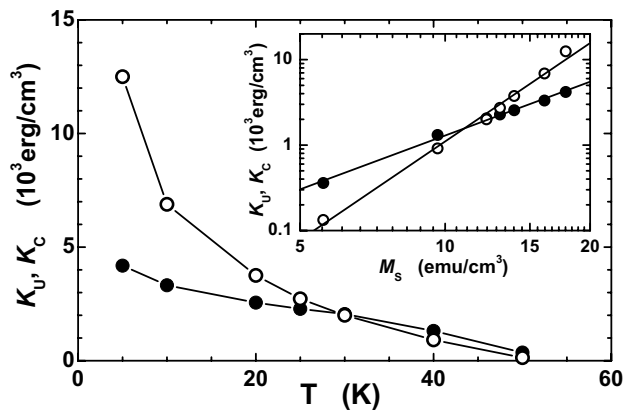


FIG. 3:  $K_U$  (bullets) and  $K_C$  (open symbols), extracted from  $M(H)$  loops, versus temperature; (inset)  $K_U$  and  $K_C$  versus saturation magnetization.

peratures, the curvature of the  $M_{[110]}(H)$  becomes small, and so the uncertainties in  $K_U$  and  $K_C$  become large. In this regime we determine  $K_C$  and  $K_U$  from the anisotropy fields at which the magnetization is fully rotated in the direction of the external magnetic field, *i.e.* when the magnetization projections  $M_{[110]}$  and  $M_{[1\bar{1}0]}$  coincide with  $M_S$ , as shown in Fig. 2. The corresponding fields are given by  $2(K_C + K_U)/M_S$  and  $2(K_C - K_U)/M_S$ , respectively. We then confirm that the obtained values are in agreement with the  $M_{[110]}(H)$  curve. The values of  $K_U$  and  $K_C$  for the studied sample are shown in Fig. 3.  $K_C$  is larger than  $K_U$  at low temperatures, but decreases more rapidly with increasing temperature, so that  $K_C \sim K_U$  at around 30 K. Therefore, a transition from biaxial to uniaxial anisotropy is expected around this point, as is observed in Fig. 1. The measured  $K_U$  and  $K_C$  allow us to obtain the easy axis direction  $\theta$  at each temperature from Eq. 1, from which we can predict the values of  $M_{[110]}$ ,  $M_{[1\bar{1}0]}$ , and  $M_{[100]}$  at remanence. These are shown by the half-filled symbols in Fig. 1, and are in agreement with the measured values, and so further endorsing the model.

$K_C$  and  $K_U$  are plotted versus  $M_S$  in the inset of Fig. 3, showing a power-law dependence with  $K_C = (0.17 \pm 0.05)M_S^{(3.8 \pm 0.2)}$  and  $K_U = (11 \pm 2)M_S^{(2.1 \pm 0.1)}$ . Thus, the uniaxial and biaxial anisotropy constants show the expected quadratic and quartic dependence on  $M_S$ , respectively [18]. The single domain model therefore provides us with a phenomenological basis for understanding the magnetization rotation of the sample, for example in response to a weak AC magnetic field.

Measurements of the real part of the AC magnetization along the [100], [110], and  $[1\bar{1}0]$  axes,  $m'_{[100]}$ ,  $m'_{[110]}$ , and  $m'_{[1\bar{1}0]}$ , in response to a 5 Oe, 11 Hz driving field, are shown in Fig. 4(a). Similar to a previous report [11], two peaks are observed in  $m'_{[100]}$ , one close to  $T_C$  and one close to the reorientation transition. These two peaks were interpreted by Hamaya *et al.* [11] as arising from ferro-

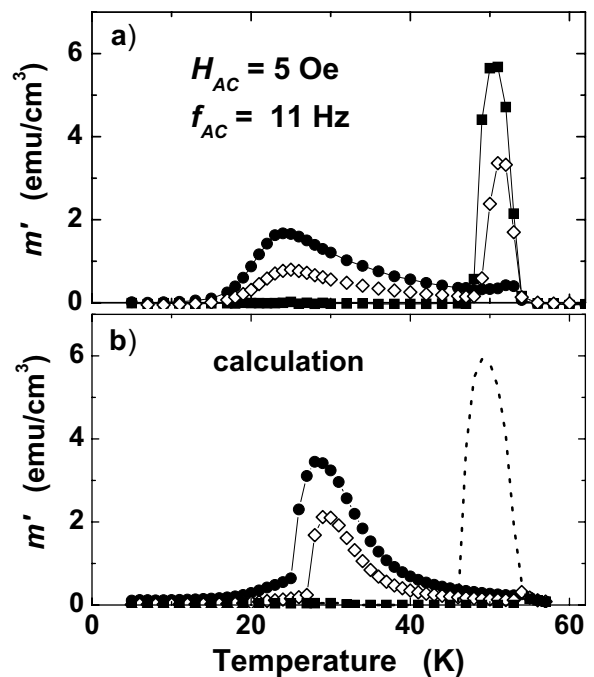


FIG. 4: Symbols as in Fig. 1. (a) real part of the AC susceptibility under a 5 Oe, 11Hz driving field, for measurements along [110],  $[1\bar{1}0]$  and [100] axes; (b) change in projected magnetization on sweeping external field from +5 Oe to -5 Oe, calculated using Eq. 1 and the measured dependence of  $K_C$  and  $K_U$  on  $M_S$ .

to paramagnetic transitions of two phase segregated distinct magnetic phases, with biaxial and uniaxial magnetic anisotropies respectively. However, Fig. 4 shows that the low  $T$  peak is not present for  $m'_{[110]}$ , while the peak close to  $T_C$  is very small for  $m'_{[110]}$ . This strong dependence of the peak amplitudes on the orientation of the driving field argues against the interpretation of Hamaya *et al.* [11], and indicates instead that the peaks result from the interplay of the biaxial and uniaxial contributions to the magnetic anisotropy. When  $K_C$  is only slightly larger than  $K_U$ , the biaxial easy axes lie close to and on either side of the  $[1\bar{1}0]$  direction, and the energy barrier separating them becomes very small. Therefore, a small magnetic field applied away from the  $[1\bar{1}0]$  direction produces a relatively large increase of the projected magnetization along the field direction, and thus a large (DC or AC) susceptibility is measured. Meanwhile, the susceptibility along the  $[1\bar{1}0]$  direction is much smaller, since a small applied field can only rotate the magnetization by the small angle between the easy axis and the  $[1\bar{1}0]$  axis. To confirm this interpretation, we perform a numerical simulation of the AC susceptibility measurement, calculating the in-phase signal  $m \sin(\omega t)$  in response to an applied field  $H \sin(\omega t)$ . The simulated results shown in Fig. 4(b) are obtained from Eq. 1 with no free parameters, using only the measured  $M_S(T)$  and the obtained power-law dependencies of  $K_C$  and  $K_U$  on  $M_S$ . Considering the

simplicity of the model, the calculation reproduces the position, shape and angle-dependence of the peak at the reorientation transition remarkably well.

The peak close to  $T_C$ , which is not reproduced by the calculation, is in small part due to the transition of the system to a paramagnetic state, but is predominantly due to the rapid decrease of the coercivity  $H_C$  close to  $T_C$ . As shown in Fig. 2(a),  $H_C = 2$  Oe for  $[1\bar{1}0]$  at 50K, so is significantly lower than the driving field. The field is therefore sufficient to produce a complete reversal of the magnetization. Equation 1 only includes coherent rotation, so overestimates the reversal field needed, which is why this peak does not appear in the calculated result. Experimentally, we obtain  $H_C \simeq (1 - T/T_C)^2 \times 150$  Oe close to  $T_C$  for the  $[1\bar{1}0]$  direction. If this is explicitly included in the numerical simulation, by forcing a  $180^\circ$  rotation of the magnetization if the driving field exceeds this value, then the peak close to  $T_C$  is reproduced [dashed line in Fig. 4(b)]. Finally, the coercivity of (Ga,Mn)As is known to be frequency-dependent [12], resulting in the frequency-dependence of the AC susceptibility near  $T_C$  reported in ref. [11].

The susceptibility peak at the reorientation transition occurs because the field required to rotate the magnetization between the biaxial easy axes becomes very small at this point. However, the energy barrier opposing a  $180^\circ$  reversal remains large. Therefore, a  $90^\circ$  rotation of the low-temperature magnetization could be achieved by heating to the reorientation temperature, followed by cooling in a weak external field. This may be important for thermally assisted writing schemes, in which a laser pulse is used to assist the magnetization reversal of a high anisotropy material, as the temperature where softening of the anisotropy occurs (and thus the laser fluence needed) may be substantially reduced by the presence of a reorientation transition. Such schemes involving  $90^\circ$  rotation have been explored only recently [20]. Since a similar combination of uniaxial plus biaxial anisotropy may be observed in systems showing room temperature ferromagnetism, such as Fe/InAs(001) [21], this may be of technological relevance.

In summary, the recently reported AC susceptibility peak at the reorientation transition temperature in (Ga,Mn)As is shown to occur even for single-phase, single-domain systems, and is a consequence of the cancellation of uniaxial and biaxial magnetic anisotropy fields. The softening of the anisotropy at the transition may be important for magnetization manipulation in spintronics devices.

Support of EPSRC, EU FENIKS (G5RD-CT-2001-0535), and Polish PBZ/KBN/044/PO3/2001 projects is gratefully acknowledged.

---

\* Electronic address: mikes@ifpan.edu.pl

- [1] H. Ohno, J. Magn. Mater. **272**, 1 (2004).
- [2] F. Matsukura, H. Ohno, T. Dietl, in: K.H.J. Buschow (Ed.), Handbook of Magnetic Materials, Vol. 14, Elsevier, Amsterdam, 2002, p. 1.
- [3] K.M. Yu, W. Walukiewicz, T. Wojtowicz, I. Kuryliszyn, X. Liu, Y. Sasaki, J.K. Furdyna, Phys. Rev. B **65**, 201303(R) (2002).
- [4] K.Y. Wang, K.W. Edmonds, R.P. Campion, B.L. Gallagher, N.R.L. Farley, C.T. Foxon, M. Sawicki, P. Boguslawski, T. Dietl, J. Appl. Phys. **95**, 6512 (2004).
- [5] K.W. Edmonds, N.R.S. Farley, T.K. Johal, G. van der Laan, R.P. Campion, B.L. Gallagher, and C.T. Foxon, Phys. Rev. B **71**, 064418 (2005).
- [6] T. Jungwirth, K.Y. Wang, J. Masek, K.W. Edmonds, J. König, J. Sinova, M. Polini, N.A. Goncharuk, A.H. MacDonald, M. Sawicki, R.P. Campion, L.X. Zhao, C.T. Foxon, and B.L. Gallagher, Phys. Rev. B (accepted), cond-mat/0505215.
- [7] T. Dietl, H. Ohno, and F. Matsukura, Phys. Rev. B **63**, 195205 (2001).
- [8] M. Abolfath, T. Jungwirth, J. Brum, and A.H. MacDonald, Phys. Rev. B **63**, 054418 (2001).
- [9] M. van Schilfgaarde and O.N. Mryasov, Phys. Rev. B **63**, 233205 (2001).
- [10] H. Raebiger, A. Ayuela, J. von Boehm, and R.M. Nieminen, J. Mag. Mag. Mater. **290**, 1398 (2005).
- [11] K. Hamaya, T. Taniyama, Y. Kitamoto, T. Fujii, and Y. Yamazaki, Phys. Rev. Lett. **94**, 147203 (2005).
- [12] D. Hrabovsky, E. Vanelle, A. R. Fert, D. S. Yee, J. P. Redoules, J. Sadowski, J. Kanski, and L. Ilver, Appl. Phys. Lett. **81**, 2806 (2002).
- [13] H. X. Tang, R. K. Kawakami, D. D. Awschalom, and M. L. Roukes, Phys. Rev. Lett. **90**, 107201 (2003).
- [14] U. Welp, V.K. Vlasko-Vlasov, X. Liu, J. K. Furdyna, and T. Wojtowicz, Phys. Rev. Lett. **90**, 167206 (2003).
- [15] X. Liu, Y. Sasaki, and J.K. Furdyna, Phys. Rev. B **67**, 205204 (2003).
- [16] M. Sawicki, F. Matsukura, A. Idziaszek, T. Dietl, G.M. Schott, C. Ruester, G. Karczewski, G. Schmidt, and L.W. Molenkamp, Phys. Rev. B, **70** 245325 (2004).
- [17] M. Sawicki, K-Y Wang, K.W. Edmonds, R.P. Campion, C.R. Staddon, N.R.S. Farley, C.T. Foxon, E. Papis, E. Kamiska, A. Piotrowska, T. Dietl, and B.L. Gallagher, Phys. Rev. B **71**, 121302(R) (2005).
- [18] H.B. Callen, and E. Callen, J. Phys. Chem. Sol. **27**, 1271 (1966).
- [19] R.P. Campion, K.W. Edmonds, L.X. Zhao, K.Y. Wang, C.T. Foxon, B.L. Gallagher, and C.R. Staddon, J. Crystal Growth **247**, 42 (2003).
- [20] G.V. Astakhov, A.V. Kimel, G.M. Schott, A.A. Tsvetkov, A. Kirilyuk, D.R. Yakovlev, G. Karczewski, W. Ossau, G. Schmidt, L.W. Molenkamp, T. Rasing, Appl. Phys. Lett., **86** 152506 (2005).
- [21] Y.B. Xu, D.J. Freeland, M. Tselepi, and J.A.C. Bland, Phys. Rev. B **62**, 1167 (2000).